

## Relaxor behaviour of $(\text{Ba}_{0.5}\text{Sr}_{0.5})(\text{Ti}_{0.6}\text{Zr}_{0.4})\text{O}_3$ ceramics

T BADAPANDA\*, S K ROUT<sup>†</sup>, S PANIGRAHI and T P SINHA<sup>††</sup>

Department of Physics, National Institute of Technology, Rourkela 769 008, India

<sup>†</sup>Department of Applied Physics, Birla Institute of Technology, Ranchi 835 215, India

<sup>††</sup>Department of Physics, Bose Institute, Kolkata 700 009, India

MS received 29 March 2008; revised 19 June 2008

**Abstract.**  $\text{Ba}_{0.5}\text{Sr}_{0.5}\text{Ti}_{0.6}\text{Zr}_{0.4}\text{O}_3$  ceramic has been prepared through solid state reaction route. X-ray diffraction shows that the sample has cubic perovskite structure with space group  $Pm-3m$  at room temperature. Temperature dependent dielectric study of the ceramic has been investigated in the frequency range 50 Hz–1 MHz. The density of the sample is determined using Archimedes' principle and is found to be ~99% of X-ray density. The dielectric study revealed diffuse phase transition of second order. A broad dielectric anomaly coupled with the shift of dielectric maxima toward a higher temperature with increasing frequency indicates the relaxor-type behaviour in the ceramics. The index of relaxation ( $\gamma$ ) and the broadening parameter ( $\Delta$ ) were estimated from a linear fit of the modified Curie–Weiss law. The value of  $\gamma \sim 1.72$  indicates the strong relaxor nature of the ceramic. A remarkably good fit to the Vogel–Fulcher relation further supports such a relaxor nature.

**Keywords.** Electroceramics; perovskites; barium–strontium–titanate–zirconate; phase formation; permittivity.

### 1. Introduction

Recently, a new wave of interest has risen on relaxor ferroelectrics with complex perovskite structure due to its wide use in fabrication of multilayer ceramic capacitors, electrostrictive actuators, and electromechanical transducers. The ferroelectric-relaxor behaviour, which is characterized by diffuse phase transition, has been studied extensively both theoretically as well as experimentally since a long time (Cross 1987). Various physical models have been proposed to explain the properties of relaxor behaviour, e.g. microscopic composition fluctuation (Smolenskii 1970), order-disorder transition (Setter and Cross 1980), microdomain and macrodomain switching (Yao *et al* 1984), ‘dipolar-glass’ model (Viehland *et al* 1990), and quenched random field model (Westphal *et al* 1992). In spite of continuous fundamental investigations on relaxor ferroelectrics in recent years, the nature of their extraordinary properties has not yet been understood completely, and they are still the subject of intensive research. It is accepted that the relaxor nature is related to the micropolar regions induced by B-site substitution, and the atomic radii and chemical valence differences of ions will often affect the relaxor effect. Most relaxor ferroelectrics belong to the family of complex lead-based perovskite oxides, such as  $\text{Pb}(\text{Mg}_{1/3}\text{Nb}_{2/3})\text{O}_3$  (PMN), which is often considered as a model system. However, these compounds

have the obvious disadvantages associated with the volatility and toxicity of  $\text{PbO}$ .

$\text{BaTiO}_3$ -based solid solutions are environment-friendly dielectrics with similar performances by as many Pb-based electroceramics. Their properties can be tuned by composition and controlling their microstructural characteristics (porosity level, grain size, secondary phases, core-shell structures, etc).  $\text{BaZr}_x\text{Ti}_{1-x}\text{O}_3$  (BZT) system is one of the most attractive material due to its phase formation mechanism (Aliouane *et al* 2005; Bera and Rout 2005), local polar characteristics (Farhi *et al* 1999) and dielectric/tunability properties for microwave applications (Weber *et al* 2001; Lee *et al* 2005).  $\text{BaTiO}_3$  (BT) is known to form complete solid solution with  $\text{BaZrO}_3$  (BZ) (i.e. BZT solid solution). It has been reported (Hennings *et al* 1982) that at ~15 atom% Zr substitution the three transition temperatures of  $\text{BaTiO}_3$ , rhombohedra to orthorhombic, orthorhombic to tetragonal and tetragonal to cubic, merge near room temperature and the doped material exhibits enhanced dielectric constant. With further increase in Zr contents beyond 15 atom %, a diffuse dielectric anomaly in ceramic has been observed with the decrease in the transition temperature (Yu *et al* 2000) and the material showed typical relaxor-like behaviour in the range 25–42 atom % Zr substitution (Yu *et al* 2002). It is well known that  $\text{SrTiO}_3$  forms complete solid solution with  $\text{BaTiO}_3$  without much decrease in dielectric permittivity. The Sr ion may take 12 co-ordination sites with eight near neighbours and four more distant ones. This modification assumes a possible displacement of Sr ion out of

\*Author for correspondence (badapanda.tanmaya@gmail.com)

the oxygen dodecahedron centre and is able to induce a dipolar moment whose occurrence leads to modification of  $T_C$ . This inspired us to work on the effect of Sr on structural and dielectric properties of  $\text{BaTi}_{0.6}\text{Zr}_{0.4}\text{O}_3$  relaxor composition prepared through solid–oxide reaction route.

## 2. Experimental

The sample was prepared through solid state reaction route. The composition was prepared from  $\text{BaCO}_3$  (S.D. Fine Chem., Mumbai),  $\text{SrCO}_3$  (S.D. Fine Chem., Mumbai),  $\text{TiO}_2$  (E. Merck India Ltd.) and  $\text{ZrO}_2$  (Loba Chem., Mumbai). All the chemicals were having more than 99% purity. The raw powder was thoroughly mixed in agate mortar using IPA. The homogenous mixture was calcined successively at  $1300^\circ\text{C}$  for 4 h,  $1400^\circ\text{C}$  for 4 h and finally  $1450^\circ\text{C}$  for 6 h with intermediate mixing and grinding. The synthesized powder was characterized with respect to phase identification and lattice parameter measurements, using  $\text{Cu}-\text{K}\alpha$  XRD (PW-1830, Philips, The Netherlands). The average grain size was measured through optical microscope. The structural refinements were carried out using Rietveld refinement program, MAUD and was reported elsewhere (Rout et al 2006). For electrical property measurements, the disks were pressed uniaxially at 200 MPa with 2 wt% PVA solution added as binder and that were sintered at  $1450^\circ\text{C}$  for 4 h. Disk density was evaluated using Archimedes principle. Silver electrodes were applied on the opposite disk faces and were heated at  $700^\circ\text{C}$  for 5 min. Dielectric measurement was carried out over a frequency range 50 Hz–1 MHz using Hioki LCR meter connected to PC. The dielectric data was collected at an interval of  $3^\circ\text{C}$  while heating at a rate of  $0.5^\circ\text{C}$  per min.

## 3. Results and discussion

Figure 1 shows the XRD pattern of the  $[(\text{Ba}_{1-x}\text{Sr}_x)(\text{Ti}_{0.6}\text{Zr}_{0.4})]\text{O}_3$  sample. At room temperature, the composition with  $x = 0$  is reported as cubic by many workers (Sciau et al 2000; Weber et al 2001; Tang et al 2004) and confirmed by our earlier publication with space group  $Pm-3m$  after Rietveld refinement of XRD data. The figure shows XRD peaks shifting towards higher angle indicating decrease in lattice parameter due to the incorporation of smaller Sr in place of higher radii Ba. This is a clear indication that the Sr is systematically dissolved in BTZ lattice in the studied composition range. Figure 2 shows the microstructures of  $\text{Ba}_{0.5}\text{Sr}_{0.5}\text{Ti}_{0.6}\text{Zr}_{0.4}\text{O}_3$  ceramics.

Figure 3 shows the temperature dependency of the permittivity of  $\text{Ba}_{0.5}\text{Sr}_{0.5}\text{Ti}_{0.6}\text{Zr}_{0.4}$  ceramic. The value of  $\epsilon'$  increases gradually to a maximum value ( $\epsilon_m$ ) with increase in temperature and then decreases smoothly indicating a phase transition. The maximum of dielectric permittivity ( $\epsilon_m$ ) and the corresponding temperature maximum ( $T_m$ )

depend upon the measurement frequency for all the compositions. The magnitude of dielectric constant decreases with increase in frequency and the maximum shifts to higher temperature. This indicates that the dielectric polarization is of relaxation type in nature. At 1 kHz, the dielectric maximum ( $\epsilon_m$ ) of pure  $\text{BaTi}_{0.6}\text{Zr}_{0.4}\text{O}_3$  is observed at 168 K ( $T_m$ ) (Rout et al 2008). The observed high value of  $T_m$  is due to higher grain size (Rout et al 2008). It is experimentally reported (Tang et al 2004) that as the grain size decreases, the maximum dielectric constant and transition temperature decrease. The effect of grain size on transition temperature originates from the higher surface tension in smaller grains which acts in the same manner as hydrostatic pressure, thus the Curie point decreases. In addition, the force experienced by the atoms and ions in the vicinity of, or far from, the surface of grain are not similar. These considerations suggest that a quadratic gradient may exist between the surface and the bulk of grains. However, for smaller grain size, the

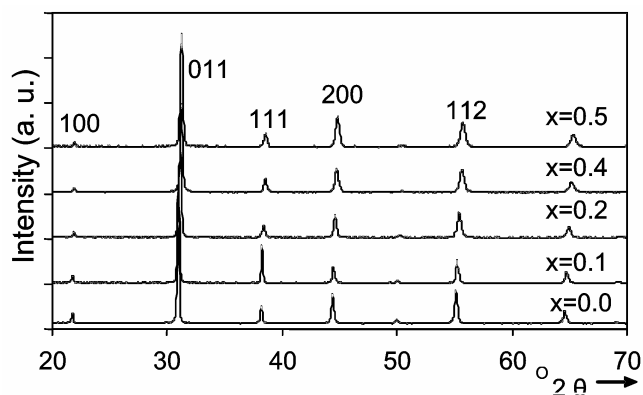


Figure 1. XRD pattern of  $\text{Ba}_{1-x}\text{Sr}_x\text{Ti}_{0.6}\text{Zr}_{0.4}\text{O}_3$  with different  $\text{Sr}(x)$  contents.

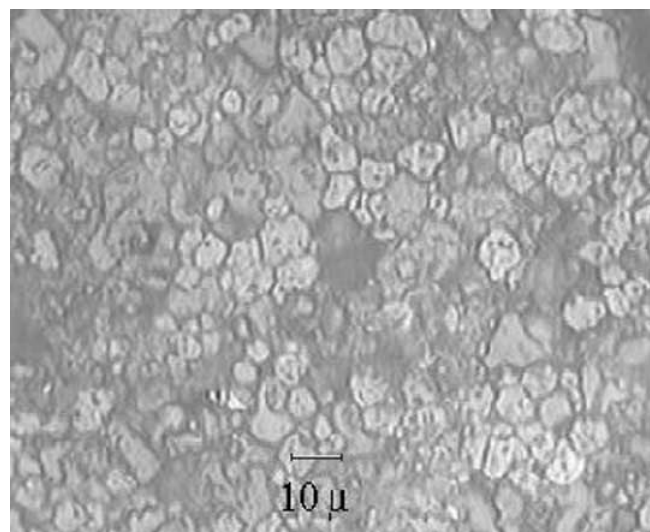


Figure 2. Microstructure of  $\text{Ba}_{0.5}\text{Sr}_{0.5}\text{Ti}_{0.6}\text{Zr}_{0.4}\text{O}_3$  ceramics.

superficial layers of the grains represent a significant fraction and may dominate in the structural and dielectric measurement. It can also be seen that the temperature corresponding to maximum permittivity,  $T_m$ , decreases with Sr content. The decrease in  $T_m$  may be due to the lower radii of Sr than Ba and smaller grain size.

It is known that the dielectric permittivity of a normal ferroelectric above the Curie temperature follows the Curie–Weiss law described by

$$\epsilon' = C/(T - T_0), \quad (T > T_C),$$

where  $T_0$  is the Curie–Weiss temperature and  $C$  the Curie–Weiss constant.

Figure 4 shows the plot of inverse dielectric constant vs temperature at different frequencies. A clear deviation

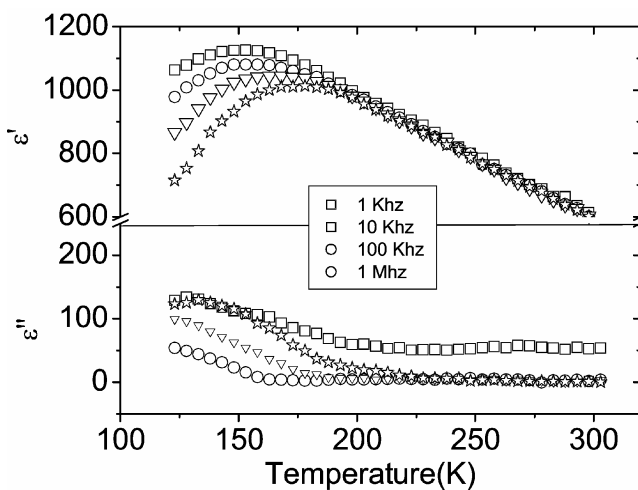


**Figure 3.** Temperature dependency of real and imaginary parts of permittivity of  $Ba_{0.5}Sr_{0.5}Ti_{0.6}Zr_{0.4}O_3$  at various frequencies.

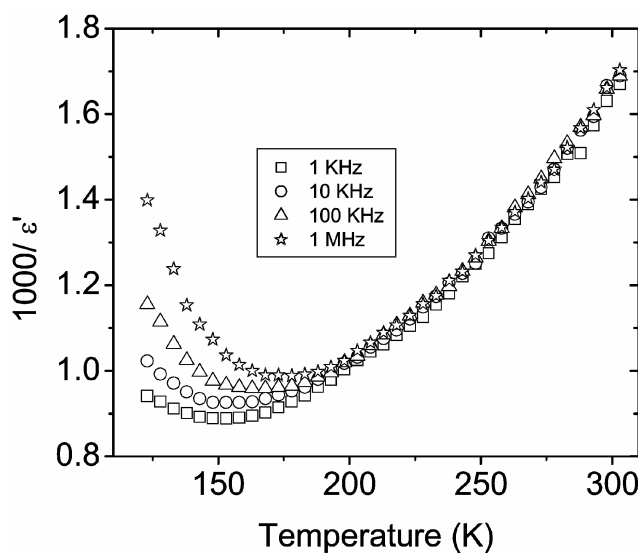


**Figure 4.** Plot of temperature dependency of  $1/\epsilon'$  for  $Ba_{0.5}Sr_{0.5}Ti_{0.6}Zr_{0.4}O_3$  at various frequencies.

from Curie–Weiss law can be seen in all representative frequencies. The parameters obtained at 1 kHz and 1 MHz are listed in table 1. The parameter,  $\Delta T_m$ , which describes the degree of the deviation from the Curie–Weiss law, is defined as

$$\Delta T_m = T_{CW} - T_m,$$

where  $T_{CW}$  denotes the temperature from which the permittivity starts to deviate from the Curie–Weiss law and  $T_m$  represents the temperature of the dielectric maximum. The Curie temperature is determined from the graph by extrapolation of the reciprocal of dielectric constant of the paraelectric region and the values obtained are given in table 1.

A modified Curie–Weiss law has been proposed by many research groups to describe the diffuseness of a phase transition as

$$\frac{1}{\epsilon'} - \frac{1}{\epsilon_m} = (T - T_m)^\gamma / C',$$

where  $\gamma$  and  $C'$  are assumed to be constants. The parameter,  $g$ , gives information on the character of the phase transition; for  $\gamma = 1$ , a normal Curie–Weiss law is obtained, for  $\gamma = 2$ , it reduces to the quadratic dependency which describes a complete diffuse phase transition. The plot of  $\log(1/\epsilon' - 1/\epsilon_m)$  vs  $\log(T - T_m)$  at 100 kHz for composition is shown in figure 4. Linear relationships are observed. The slopes of the fitting curve are used to determine the parameter  $\gamma$  value. The values of  $\gamma$  at 100 kHz are found to be 1.72 indicating transitions are of diffuse type. The value of  $\gamma$  shows that the material is highly disordered. The decreased value of  $\gamma$  with Sr content indicates decrease in diffusivity. The broadened dielectric maximum (in  $\epsilon'$  vs temperature curve) and its deviation from Curie–Weiss law are the main characteristics of a diffuse phase transition of the material. The diffuse phase transition and deviation from Curie–Weiss type may be assumed due to disordering. The broadness in  $\epsilon'$  vs temperature curve is one of the most important characteristics of the disordered perovskite structure with diffuse phase transition. The broadness or diffusiveness occurs mainly due to compositional fluctuation and structural disordering in the arrangement of cation in one or more crystallographic sites of the structure. This suggests a microscopic heterogeneity

**Table 1.** Parameters obtained from temperature dependency dielectric study on the composition,  $Ba_{0.5}Sr_{0.5}Ti_{0.6}Zr_{0.4}O_3$  at different frequencies.

	1 kHz	10 kHz	100 kHz	1 MHz
$T_m$ (K)	152.53	157.65	167.23	177.84
$T_0$ (K)	170.471	179.453	187.81	192.88
$C (10^5 \text{ K})$	1.4	1.56	1.71	1.95
$\Delta T_m$	64.98	65.7	70.47	80.7
$T_{CW}$	217.51	223.35	237.701	257.88
$\epsilon_m$	1132.88	1008.942	1048.314	1010.742

in the compound with different local Curie points. The nature of the variation of dielectric constant and non-polar space group suggests that the material may have ferroelectric phase transition.

The broadening of the phase transition is better illustrated by plotting the reduced dielectric constant ( $\varepsilon'/\varepsilon_m$ ) as a function of reduced temperature,  $\tau$  [=  $(T - T_m)/T_m$ ] at different frequencies (figure 6). The full width of the plot has very little dispersion over a wide frequency range similar to the observation made in other relaxor materials (Tyunina et al 1999).

The plot of  $\log(\nu)$  vs  $1/T_m$  is shown in figure 7. The nonlinear nature indicates that the data cannot be fitted with a simple Debye equation. Therefore, the relaxation time in ceramics can be expressed by Vogel–Fulcher law (Uchino and Nomura 1982; Pantou et al 2003). In order

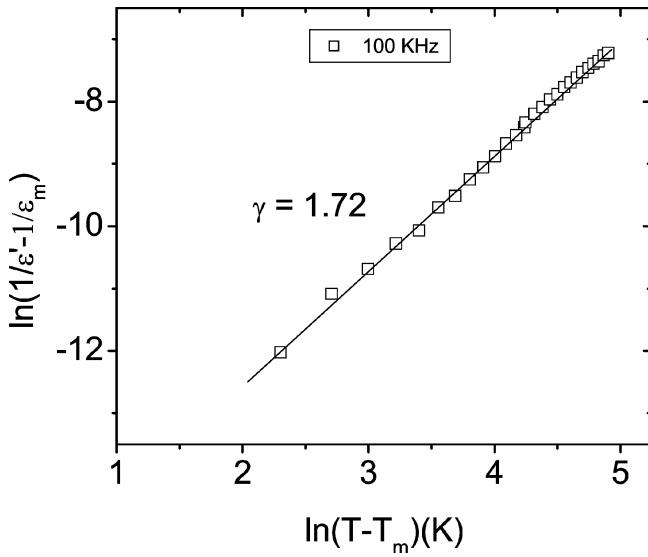


Figure 5. Plot of  $\log(1/\varepsilon' - 1/\varepsilon_m)$  vs  $\log(T - T_m)$  of  $\text{Ba}_{0.5}\text{Sr}_{0.5}\text{Ti}_{0.6}\text{Zr}_{0.4}\text{O}_3$  at 100 kHz.

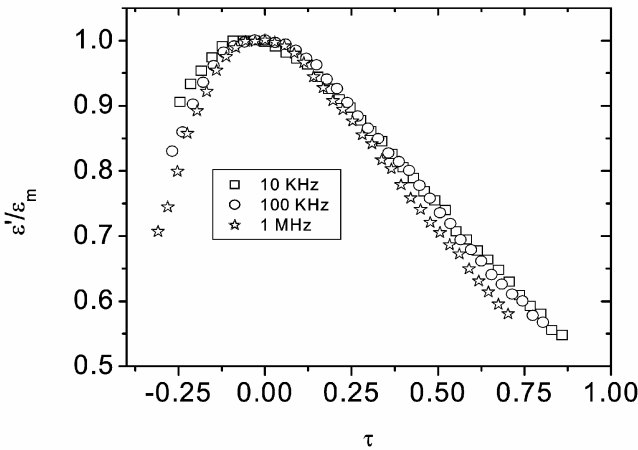


Figure 6. Plot of reduced dielectric constant,  $\varepsilon'/\varepsilon_{\max}$  vs reduced temperature,  $\tau$  [=  $(T - T_m)/T_m$ ] in the frequency range 10 kHz–1 MHz.

to analyse the relaxation features, i.e. relation between  $\nu$  and  $T_m$  of the ceramics, the experimental curves were fitted using the Vogel–Fulcher formula (Guo et al 2004; Kleemann 1993)

$$\nu = \nu_0 \exp\left[\frac{-E_a}{k_B(T_m - T_f)}\right],$$

where  $\nu_0$  is the attempt frequency,  $E_a$  the measure of average activation energy,  $k_B$  the Boltzmann constant, and  $T_f$  the freezing temperature.  $T_f$  is regarded as the temperature where the dynamic reorientation of the dipolar cluster polarization can no longer be thermally activated. The fitting curve is shown in figure 6. The fitting parameters for the composition are:  $E_a = 0.1132$  eV,  $T_f = 103$  K,  $\nu_0 = 7.9 \times 10^{11}$  Hz. The fitting parameter having close agreement with the data of V–F relationship suggests that the relaxor behaviours in the systems are analogous to that of a dipolar glass with polarization fluctuations above a static freezing temperature. The activation energy and pre-exponential factor are both consistent with thermally activated polarization fluctuations. The empirical relaxation strength describing the frequency dispersion of  $T_m$  is defined as

$$\Delta T_{\text{res}} = T_{m(1 \text{ MHz})} - T_{m(10 \text{ kHz})},$$

where  $\Delta T_{\text{res}}$  was derived from the dielectric measurement of the ceramics. The value of  $\Delta T_{\text{res}}$  is found to be 20.19.

The relaxor behaviour as observed in this ceramics can be induced by many reasons such as microscopic compositions fluctuation, the merging of micropolar regions into macropolar regions, or a coupling of order parameter and local disorder mode through the local strain. Vugmeister and Glinichuk reported that the randomly distributed electrical field of strain field in a mixed oxide system

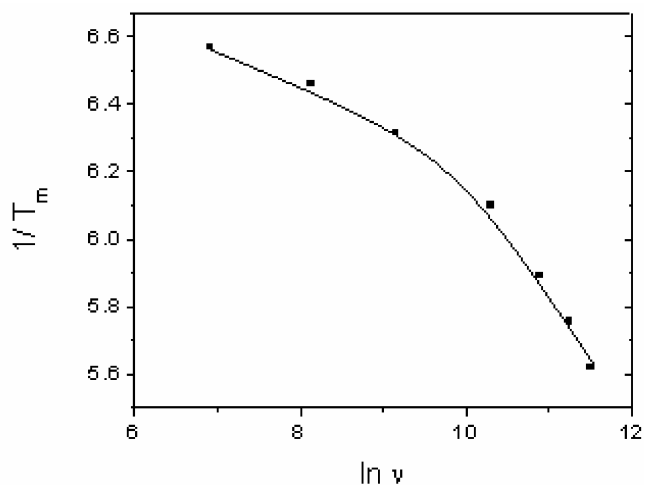


Figure 7. Plot of  $\ln(\nu)$  vs  $1/T_m$  as a function of the measured frequency of  $\text{Ba}_{0.5}\text{Sr}_{0.5}\text{Ti}_{0.6}\text{Zr}_{0.4}\text{O}_3$ . The symbols are the experimental points and line is corresponding fitting to the Vogel–Fulcher relationship.

is the main reason leading to the relaxor behaviour. In the studied composition of solid solutions,  $Ba_{0.5}Sr_{0.5}Ti_{0.6}Zr_{0.4}O_3$ , Ba and Sr ions occupy the A-sites of the  $ABO_3$  perovskite structure and Zr and Ti ions occupy the B-site. As previously mentioned, both Ti and Zr are ferroelectrically active and these cations are off-centred in the octahedral site giving rise to a local dipolar moment. In perovskite type compounds the relaxor behaviour appears when atleast two cations occupy the same crystallographic site A or B. The ionic radius of  $Zr^{4+}$  (0.98 Å) is larger than that of  $Ti^{4+}$  (0.72 Å). Therefore, an inhomogeneous distribution results at the B-site of the structure. A cationic disorder induced by B-site substitution is always regarded as the main derivation of relaxor behaviour. However, according to our present results, it implies that the observed higher relaxation strength attributes a cationic disorder induced by both A-site and B-site substitutions. Different effects of A-site substitution on cation ordering and the stability of the polar region are considered to be based on the polarizability of cations and the tolerance factor of the perovskite structure. For perovskites with the general formula of  $ABO_3$ , the following equation can be used to calculate the tolerance factor ( $t$ ) (Viehland *et al* 1991)

$$t = (R_A + R_O)/\sqrt{2}(R_B + R_O),$$

where  $R_A$  is the radius of A,  $R_B$  the radius of B and  $R_O$  the radius of O. As  $t$  increases, the normal ferroelectric phase becomes stabilized. So  $Ba^{2+}$  cations can stabilize the normal ferroelectrics due to the larger ionic diameter and higher polarizability. While  $Sr^{2+}$  cations in A-sites behave as a typical destabilizer against normal ferroelectrics and induces paraelectric behaviour due to smaller ionic diameter and lower polarization. In this case more macrodomains (long-range ordered regions) in Sr substituted ceramics will breakup into micropolar regions than that in pure BTZ ceramics. Mechanical stress in the grain, which is one of the causes of relaxor behaviour in the Ti and Zr mixed composition (Hennings *et al* 1982; Vugmeister and Glinichuk 1990; Viehland *et al* 1991; Pantou *et al* 2003). Stresses were introduced into the lattice during cooling after sintering process, which is due to transition from a cubic to rhombohedral phase below the Curie temperature (Hennings *et al* 1982). On the other hand, it is known that  $BaZrO_3$  shows non-ferroelectric (cubic paraelectric phase) behaviour at all temperatures because, Zr ion locates at central equilibrium position of the  $BaZrO_3$  lattice. In this case, the macrodomain in  $BaTiO_3$  could be divided into the microdomains which probably cause the relaxor behaviour. The observed high value of  $\gamma$  and relaxation strength are due to the large difference in ionic radius of  $Ba^{2+}$  (2.78 Å) and  $Sr^{2+}$  (1.32 Å) at the A-site of the perovskite structure.

#### 4. Conclusions

Perovskite  $Ba_{0.5}Sr_{0.5}Ti_{0.6}Zr_{0.4}O_3$  ceramic has been prepared through solid state reaction route. The room temperature XRD study suggests that the composition has single phase cubic symmetry with space group  $Pm-3m$ . Dielectric study of the composition shows typical relaxor like behaviour far below room temperature. The experimental  $T_m$  data points are in good agreement with the Vogel–Fulcher relation. The quantitative characterization of the relaxor behaviour based on empirical parameters ( $\Delta T_m$ ,  $\Delta T_{res}$  and  $\Delta T_{CW}$ ) confirms the relaxor behaviour of the composition,  $Ba_{0.5}Sr_{0.5}Ti_{0.6}Zr_{0.4}O_3$ .

#### References

- Aliouane K, Guehria-Laidoudi A, Simon A and Ravez J 2005 *Solid State Ionics* **7** 1324
- Bera J and Rout S K 2005 *Mater. Lett.* **59** 135
- Cross L E 1987 *Ferroelectrics* **76** 241
- Farhi R, Marssi E I, Simon M A and Ravez J 1999 *Eur. Phys. J. B9* 599
- Guo Y, Kakimoto K and Ohsato H 2004 *Solid State Commun.* **129** 274
- Hennings D, Schell H and Simon G 1982 *J. Am. Ceram. Soc.* **65** 539
- Kleemann W 1993 *Int. J. Mod. Phys. B7* 2469
- Lee S J, Kwak M H, Moon S E, Ryu H C, Kim Y T and Kang K Y 2005 *Integr. Ferroelectr.* **77** 93
- Pantou R, Dubourdieu C, Weiss F, Kreisel J, Kobernik G and Haessler W 2003 *Mater. Sci. Semicond. Process* **5** 237
- Rout S K, Sinha E, Panigrahi S, Bera J and Sinha T P 2006 *J. Phys. Chem. Solids* **67** 2257
- Rout S K, Barhai P K and Sinha E 2008 *Phase Trans.* **81** 129
- Sciau Ph, Calvarin G and Ravez J 2000 *Solid State Commun.* **113** 77
- Setter N and Cross L E 1980 *J. Appl. Phys.* **51** 4356
- Smolenskii G A 1970 *J. Phys. Soc. Jpn* **28** 26
- Tang X G, Wang J, Wang X X and Chan H L W 2004 *Solid State Commun.* **131** 163
- Tyunina M, Levoska J, Sternberg A and Leppavuori S 1999 *J. Appl. Phys.* **86** 5179
- Uchino K and Nomura S 1982 *Ferroelectr. Lett.* **44** 55
- Viehland D, Jang S J, Cross L E and Wuttig M 1990 *J. Appl. Phys.* **68** 2916
- Viehland D, Wuttig M and Cross L E 1991 *Ferroelectrics* **120** 71
- Vugmeister B E and Glinichuk M D 1990 *Rev. Mod. Phys.* **62** 993
- Westphal V, Kleemann W and Glinichuk M D 1992 *Phys. Rev. Lett.* **68** 2916
- Weber U *et al* 2001 *J. Am. Ceram. Soc.* **84** 759
- Yao X, Chen Z L and Cross L E 1984 *J. Appl. Phys.* **54** 3399
- Yu Z, Guo R and Bhalla A S 2000 *J. Appl. Phys.* **88** 410
- Yu Z, Guo R and Bhalla A S 2002 *Appl. Phys. Lett.* **81** 1285